

(found) for  $C_{47}H_{54}BMoO_3P$ : C, 70.15 (70.32); H, 6.76 (6.68).

$Cp(OC)_2Mo(Ph_2PCOCH_2CH_2CH_2)$  (**9a**). To a solution of **7a** (0.191 g) in  $CH_2Cl_2$  (6 mL) was added Proton Sponge (0.69 g, 1.34 equiv). The solvent was removed (in vacuo) and the residue column chromatographed on Fluorisil by eluting with  $CH_2Cl_2$ -hexane (50:50). Addition of hexane to the eluate precipitated **9a** as a yellow powder (0.063 g, 55%). Anal. Calcd (found) for  $C_{23}H_{21}MoO_3P$ : C, 58.49 (57.91); H, 4.48 (4.57).  $^1H$  NMR: Cp,  $\delta$  5.24 (singlet);  $OCH_2$ ,  $\delta$  3.98 (1:3:3:1 quartet);  $CCH_2$ ,  $\delta$  3.29 (broad multiplet);  $CH_2CH_2CH_2$ ,  $\delta$  2.31 (broad multiplet). Complexes **9b** and **9c** could be prepared in similar yields from **8b** and **7c**. Reaction of **8b** with Proton Sponge required 3 h at 20 °C, probably because of a high activation energy associated with a trans to cis isomerization prior to the formation of **9b**. Anal. Calcd (found) for  $C_{23}H_{33}MoO_3P$  (**9b**): C, 57.03 (56.62); H, 6.87 (6.55). Calcd (found) for  $C_{17}H_{23}MoO_3P$  (**9c**): C, 50.76 (50.34); H, 5.76 (5.40).

$[Cp(OC)_2Mo(\mu-PPH_2)(\mu-H)Pt(COCH_2CH_2CH_2)(PCy_3)]-BPh_4$  (**10a**).  $Pt(C_2H_4)_2(PCy_3)$  (0.176 g, 0.33 mmol) was added to a solution of **7a** (0.273 g, 0.34 mmol) in  $CH_2Cl_2$  (10 mL). After 1 h the solvent was removed (in vacuo) and the residue redissolved in a minimum volume of acetone. Addition of hexane gave **10a** as a yellow powder (0.360 g, 83% yield). Recrystallization from

$CH_2Cl_2$ -hexane gave yellow prisms suitable for X-ray diffraction. Anal. Calcd (found) for  $C_{85}H_{75}BMoO_3P_2Pt \cdot CH_2Cl_2$ : C, 58.59 (58.13); H, 5.96 (5.89). The cationic dimers **10b** and **10c** were similarly prepared (70-80% yields). Anal. Calcd (found) for  $C_{85}H_{87}BMoOP_2Pt$  (**10b**): C, 60.98 (60.73); H, 6.85 (6.62). Complex **10b** exhibited an unusually large separation of the diastereotopic  $OCH_2$  proton resonances.  $^1H$  NMR: Cp,  $\delta$  5.39;  $OCH_2$ ,  $\delta$  4.98 and 4.76 (broad multiplets);  $CCH_2$ ,  $\delta$  3.48 and 3.38 (broad multiplets);  $CH_2CH_2CH_2$ , resonances masked by Cy proton resonances.

The reactions of **7** and **8** with  $Pt(C_2H_4)(PPh_3)_2$  were carried out in NMR tubes ( $CD_2Cl_2$  solutions). Attempts to separate **13** and **14** were not completely successful.

**Acknowledgment.** We thank the Natural Sciences and Engineering Research Council of Canada for financial support.

**Supplementary Material Available:** Tables A-C, containing hydrogen atom positions, anisotropic thermal parameters, and bond lengths and bond angles in the cyclohexyl and phenyl groups and  $BPh_4^-$  anion (4 pages); Table D, containing final structure factor amplitudes (15 pages). Ordering information is given on any current masthead page.

## Reactions of $HC\equiv CMe_2NHCOR$ Alkynes with $M_3(CO)_{12}$ Carbonyls ( $M = Ru, R = C_6H_9, Ph; M = Os, R = C_6H_9$ ). Synthesis and Crystal Structure of $Ru_4(CO)_{11}(HC\equiv CMe_2NHCOC_6H_9)$ , a Butterfly Cluster Showing an Interaction between a Wingtip Metal and the Amide CO

Giovanni Predieri, Antonio Tiripicchio,\* and Marisa Tiripicchio Camellini

*Istituto di Chimica Generale ed Inorganica, Università di Parma, Centro di Studio per la Strutturistica  
Diffraattometrica del CNR, Viale delle Scienze, I-43100 Parma, Italy*

Mirco Costa

*Istituto di Chimica Organica, Università di Parma, Viale delle Scienze, I-43100 Parma, Italy*

Enrico Sappa

*Dipartimento di Chimica Inorganica, Chimica Fisica e Chimica dei Materiali, Università di Torino,  
Via P. Giuria 7, I-10125 Torino, Italy*

Received June 26, 1989

The alkynes  $HC\equiv CMe_2NHCOR$  react with  $M_3(CO)_{12}$  ( $M = Ru$  or  $Os$ ) giving, upon oxidative addition, the expected hydrides  $(\mu-H)M_3(CO)_9(\mu_3-\eta^2-C\equiv CMe_2NHCOR)$  and the unprecedented butterfly clusters  $M_4(CO)_{11}(\mu_4-\eta^2-HC\equiv CMe_2NHCOR)$ . These complexes have been characterized by spectroscopic studies; the structure of the ruthenium butterfly cluster with  $R = C_6H_9$  has been determined by X-ray diffraction methods. Crystals, containing  $CHCl_3$  as solvation molecules, are triclinic with  $Z = 2$  in a unit cell of dimensions  $a = 13.521$  (6),  $b = 14.617$  (6),  $c = 9.049$  (5) Å,  $\alpha = 79.28$  (2),  $\beta = 108.79$  (2),  $\gamma = 111.85$  (2)°. The structure has been solved from diffractometer data by direct and Fourier methods and refined by full-matrix least-squares to  $R = 0.0425$  for 4586 observed reflections. The organic ligand interacts with all the metals of the butterfly cluster in a  $\mu_4-\eta^2$  fashion through the alkyne moiety and with a wingtip metal through the amide CO group. Evidence has been obtained for the formation of the butterfly clusters via metal fragment condensation on the  $HM_3(CO)_9(C\equiv CMe_2NHCOR)$  clusters, which may be obtained in a retrosynthetic pattern via protonation of the butterfly derivatives.

### Introduction

The reactions of  $Ru_3(CO)_{12}$  with alkynes lead to different cluster substitution products depending on the nature of the alkyne;<sup>1</sup> for example, with  $C_2Ph_2$ , the butterfly cluster  $Ru_4(CO)_{12}(\mu_4-\eta^2-C_2Ph_2)$  (**1**)<sup>2</sup> is obtained via "metal fragment

condensation", whereas other internal aliphatic alkynes such as  $C_2Et_2$  undergo oxidative addition and form isomeric (allenic or allylic)  $HRu_3(CO)_9(C_6H_9)$  derivatives.<sup>3</sup>

(2) Johnson, B. F. G.; Lewis, J.; Reichert, B.; Schorpp, K. T.; Sheldrick, G. M. *J. Chem. Soc., Dalton Trans.* 1977, 1417.

(3) Gervasio, G.; Osella, D.; Valle, M. *Inorg. Chem.* 1976, 15, 1221, and references therein.

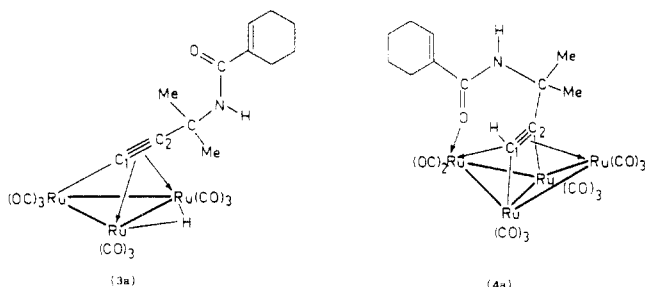
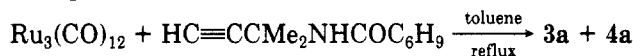
(1) Sappa, E.; Tiripicchio, A.; Braunstein, P. *Chem. Rev.* 1983, 83, 203.

Terminal alkynes, in particular *tert*-butylacetylene  $\text{HC}\equiv\text{C}\text{Bu}^t$ , also undergo oxidative addition involving the terminal hydrogen; the hydride  $(\mu\text{-H})\text{Ru}_3(\text{CO})_9(\mu_3\text{-}\eta^2\text{-C}_2\text{Bu}^t)$  (**2**), a very stable complex, is obtained in high yields.<sup>4</sup>

As a part of our studies on alkyne cluster interactions, we have examined the behavior of  $\text{Ru}_3(\text{CO})_{12}$  (and in part of  $\text{Os}_3(\text{CO})_{12}$ ) toward the functionalized alkynes *N*-( $\alpha,\alpha$ -dimethylpropargyl)-1-cyclohexenecarboxamide,  $\text{HC}\equiv\text{CCMe}_2\text{NHCOC}_6\text{H}_9$  (ligand A) and *N*-( $\alpha,\alpha$ -dimethylpropargyl)-1-benzenecarboxamide,  $\text{HC}\equiv\text{CCMe}_2\text{NHCOPh}$  (ligand B); these "modified" *tert*-butylalkynes are useful synthons for the homogeneously catalyzed synthesis of organic molecules by transition metals.<sup>5</sup> However, the interactions of these alkynes with metals and, in particular, with metal clusters, are still partly unknown.

We have found that the hydrides  $(\mu\text{-H})\text{M}_3(\text{CO})_9(\mu_3\text{-}\eta^2\text{-C}\equiv\text{CCMe}_2\text{NHCOR})$  ( $\text{M} = \text{Ru}$ ,  $\text{R} = \text{C}_6\text{H}_9$  (**3a**);  $\text{M} = \text{Ru}$ ,  $\text{R} = \text{Ph}$  (**3b**);  $\text{M} = \text{Os}$ ,  $\text{R} = \text{C}_6\text{H}_9$  (**3c**)), structurally analogous to **2**, were obtained first, as expected, via oxidative addition of the terminal alkynes to the three-metal clusters; when the reactions proceed further, "metal fragment condensation" occurs unexpectedly to give good yields of the butterfly clusters  $\text{M}_4(\text{CO})_{11}(\mu_4\text{-}\eta^2\text{-HC}\equiv\text{CCMe}_2\text{NHCOR})$  ( $\text{M} = \text{Ru}$ ,  $\text{R} = \text{C}_6\text{H}_9$  (**4a**);  $\text{M} = \text{Ru}$ ,  $\text{R} = \text{Ph}$  (**4b**);  $\text{M} = \text{Os}$ ,  $\text{R} = \text{C}_6\text{H}_9$  (**4c**), trace amounts).

The reaction for  $\text{M} = \text{Ru}$  and  $\text{R} = \text{C}_6\text{H}_9$ , and the schematic structures of the obtained compounds, **3a** and **4a**, are represented below.



The structure of **4a** has been determined by X-ray diffraction methods; the metals are in a butterfly arrangement with the alkyne coordinated to the four metals and disposed nearly parallel to the hinge, in a very classical fashion.<sup>6</sup> However, the structure of **4a** differs from that of most of the other known alkyne-containing butterfly clusters because of the bonding interaction of the oxygen atom of the amide CO group with the wingtip ruthenium atom.

Attempts at evidencing the reaction sequence leading to **4a** have been made; also some protonation reactions of this complex, relevant for its formation and decomposition, are discussed.

## Experimental Section

**General Experimental Details. Materials: Purification and Analysis of the Products.** Propargylamides  $\text{HC}\equiv\text{CCMe}_2\text{NHCOC}_6\text{H}_9$  (ligand A) and  $\text{HC}\equiv\text{CCMe}_2\text{NHCOPh}$  (ligand B) were prepared by conventional methods<sup>7</sup> using *N*-( $\alpha,\alpha$ -dimethylpropargyl)amine and benzoyl chloride or cyclo-

hexene-1-carboxylic acid chloride, obtained by commercially available cyclohexene-1-carboxylic acid and  $\text{SOCl}_2$ . *N*-( $\alpha,\alpha$ -dimethylpropargyl)amine was prepared from  $\alpha,\alpha$ -dimethylpropargyl chloride,<sup>8</sup> obtained from propargyl alcohol, commercially available, and  $\text{NH}_3$ , according to the method reported by Hennion and Teach.<sup>9a</sup>

**Melting Points and Spectroscopic Data of the Ligands A and B.** Ligand A: white solid, crystallized from dichloroethane, mp 110–111 °C; IR (KBr) 3280, 3260, 3050, 2990, 2940, 2120, 1660, 1630, 1530, 1360, 1310, 940, 930, 690, 635  $\text{cm}^{-1}$ ;  $^1\text{H}$  NMR ( $\text{CDCl}_3$ )  $\delta$  1.52–1.69 (m, 4 H, 2  $\text{CH}_2$ ), 1.63 (s, 6 H, 2 Me), 2.09–2.21 (m, 4 H, 2 allylic  $\text{CH}_2$ ), 2.31 (s, 1 H,  $\equiv\text{CH}$ ), 5.71 (br s, 1 H, NH), 6.55–6.62 (m, 1 H,  $\equiv\text{CH}$ );  $^{13}\text{C}$  NMR ( $\text{CDCl}_3$ )  $\delta$  21.50, 22.14, 24.19, 25.35 (4 C, 4  $\text{CH}_2$ ), 28.97 (2 C, 2 Me), 47.37 (1 C,  $\text{CMe}_2$ ), 68.99 (1 C,  $\equiv\text{CH}$ ), 87.44 (1 C,  $\equiv\text{C}$ ), 133.47 (1 C,  $\equiv\text{CH}$ ), 133.57 (1 C,  $\equiv\text{C}$ ), 167.67 (1 C,  $\equiv\text{CO}$ ). Anal. Calcd for  $\text{C}_{12}\text{H}_{17}\text{NO}$ : C, 75.39; H, 8.90; N, 7.33. Found: C, 75.01; H, 8.88; N, 7.08. Ligand B (although this compound is known,<sup>9b</sup> we report some spectral data for comparison with those in the clusters): white solid, crystallized from dichloroethane, mp 148 °C; IR (KBr) 3310, 3260, 3090, 3000, 1655, 1560, 1375, 1340, 1040, 960, 890, 815, 720, 710, 640  $\text{cm}^{-1}$ ;  $^1\text{H}$  NMR ( $\text{CDCl}_3$ )  $\delta$  1.76 (s, 6 H, 2 Me), 2.39 (s, 1 H,  $\equiv\text{CH}$ ), 6.20 (br s, 1 H, NH), 7.34–7.51 (m, 3 H, Ar H), 7.69–7.80 (m, 2 H, Ar H).

The  $\text{M}_3(\text{CO})_{12}$  carbonyls ( $\text{M} = \text{Ru}$  or  $\text{Os}$ ) were commercial products (Strem Chemicals) and were used as received. The reactions of the metal carbonyls with ligands A and B were performed in conventional glassware, in toluene (dehydrated over sodium) as a solvent, and under a dry  $\text{N}_2$  atmosphere; the reaction mixtures, filtered under  $\text{N}_2$ , were brought to a small volume under reduced pressure and purified on preparative TLC plates (Kieselgel P.F. Merck as solid phase; due to the high polarity of the alkyne substituents a 50:50 vol/vol mixture of light petroleum and diethyl ether was used as standard eluent). The products were analyzed by a F & M 185 C, H, N analyzer; the metal analyses were performed by Pascher Laboratories, Remagen, West Germany. The IR spectra were obtained on a Perkin-Elmer 580 B instrument; the  $^1\text{H}$  and  $^{13}\text{C}$  NMR spectra were recorded on JEOL JNM 270 FT and on Bruker CXP200 instruments.

**Synthesis of the Complexes.** The reaction of  $\text{Ru}_3(\text{CO})_{12}$  (200 mg, 0.31 mmol) with an excess of alkyne A (250 mg, 1.34 mmol) in refluxing toluene for 10 min gives a dark brown limpid solution which, after TLC purification, yields about 20% of unreacted  $\text{Ru}_3(\text{CO})_{12}$  and about 20% each of yellow **3a** and red **4a**, together with some decomposition. Similar results and yields of yellow **3b** and red **4b** are obtained from  $\text{Ru}_3(\text{CO})_{12}$  and alkyne B, in the same molar amounts and in comparable reaction conditions. Treatment of  $\text{Os}_3(\text{CO})_{12}$  (100 mg, 0.11 mmol) with alkyne A (100 mg, 0.53 mmol) in refluxing toluene for 25 min gives a dark yellow, limpid solution, which, on cooling deposits considerable amounts of unreacted  $\text{Os}_3(\text{CO})_{12}$  (these fractions were reacted further, and this has been accounted for the calculated overall yields); after TLC purification, some more unreacted  $\text{Os}_3(\text{CO})_{12}$  was collected, together with about 15% of light yellow **3c** and trace amounts of red **4c**, together with a very small decomposition. The physical characteristics and the analytical and IR data for the complexes are given in Table I, the  $^1\text{H}$  and  $^{13}\text{C}$  NMR spectra (except for **4c**) in Table II.

**Other Reactions.** No color changes were observed when a solution of **3a** in toluene was refluxed for 25 min under  $\text{N}_2$ ; after purification 98% of **3a** was recovered unaltered and only 2% of a yellow, still unidentified product was observed. By contrast, treatment of **3a** in refluxing toluene under  $\text{N}_2$  for 10 min in the presence of a 2:1 molar excess of  $\text{Ru}_3(\text{CO})_{12}$  gives a dark brown limpid solution, which deposits some  $\text{Ru}_3(\text{CO})_{12}$  upon cooling; after TLC purification, about 20% of unreacted  $\text{Ru}_3(\text{CO})_{12}$ , about 5% of unreacted **3a**, and about 30% of **4a** are recovered.

**X-ray Data Collection, Structure Determination, and Refinement for  $\text{Ru}_4(\text{CO})_{11}(\text{HC}\equiv\text{CCMe}_2\text{NHCOC}_6\text{H}_9)_2 \cdot \frac{1}{2}\text{CHCl}_3$  (**4a**).** Crystals of **4a** were obtained by slowly cooling at  $-15$  °C a heptane- $\text{CHCl}_3$  solution of the complex kept under  $\text{N}_2$ . A crystal

(4) Sappa, E.; Gambino, O.; Milone, L.; Cetini, G. *J. Organomet. Chem.* **1972**, *39*, 169. Catti, M.; Gervasio, G.; Mason, S. A. *J. Chem. Soc., Dalton Trans.* **1977**, 2260.

(5) Chiusoli, G. P.; Costa, M.; Pergrefi, P.; Reverberi, S.; Salerno, G. *Gazz. Chim. Ital.* **1985**, *115*, 691.

(6) Sappa, E.; Tiripicchio, A.; Carty, A. J.; Toogood, G. E. *Prog. Inorg. Chem.* **1987**, *35*, 437.

(7) Vogel, A. I. *A Text-book of Practical Organic Chemistry*, 3rd ed.; Longmans: Harlow, Essex, U.K., 1959; pp 401–406.

(8) Hennion, G. F.; Boisselle, A. B. *J. Org. Chem.* **1961**, *26*, 725.

(9) (a) Hennion, G. F.; Teach, E. G. *J. Am. Chem. Soc.* **1953**, *75*. (b) Swithenbank, C.; McNulty, P. J.; Viste, K. L. *J. Agric. Food Chem.* **1971**, *19*, 417–21.

Table I. Physical Characteristics, Elemental Analyses, and IR Spectra of the Complexes

complex	physical characteristics	elem. anal. <sup>a</sup>	IR (ν <sub>CO</sub> ), cm <sup>-1</sup>
3a	light yellow crystalline solid	C 34.0 (33.7), H 2.31 (2.29), N 1.90 (1.87), Ru 40.5 (40.76)	2101 m, 2075 vs, 2057 vs, 2030–2026 vs (b), 1995 m (b), <sup>b</sup> 1665 s
3b	light yellow crystalline solid	C 34.0 (33.88), H 1.9 (1.76), N 1.6 (1.87), Ru 41.0 (40.76)	2089 s, 2063 vs, 2044 vs, 2016 vs (b), 1990 s (b), <sup>b</sup> 1670 s
3c	pale yellow crystalline solid	C 25.1 (24.87), H 1.8 (1.69), N 1.5 (1.38), Os 53.0 (56.27)	2103 m, 2078 vs, 2054 vs, 2022 vs (b), 2012 (sh), 1989 s (sh), <sup>c</sup> 1690 s
4a	deep red crystals	C 30.0 (30.48), H 2.0 (1.89), N 1.8 (1.54), Ru 45.1 (44.89)	2079 s, 2044 vs, 2028 vs, 2016 s (sh), 1998 s (sh), 1992 s, 1978 m, 1962 m, <sup>b</sup> 1640 s
4b	deep red solid	C 30.5 (30.62), H 1.5 (1.45), N 1.6 (1.55), Ru 44.9 (45.09)	2069 s, 2034 vs, 2016 vs, 2004 s (sh), 1994–1983 s (b), <sup>b</sup> 1660 s
4c	deep red solid	C 22.0 (21.92), H 1.4 (1.36)	2097 m, 2050 vs, 2024 vs, 1996 s (sh, b), 1963 m (b), <sup>b</sup> 1665 vs

<sup>a</sup> Calculated values in parentheses. <sup>b</sup> Hexane–CHCl<sub>3</sub>; b = broad. <sup>c</sup> Hexane.

Table II. <sup>1</sup>H and <sup>13</sup>C NMR Spectral Data for Complexes 3 and 4<sup>c</sup>

complex	NMR	δ
3a	<sup>1</sup> H	-21.07 (s, 1 H, μH); 1.62 (m, 4 H, 2 CH <sub>2</sub> ); 1.90 (s, 6 H, 2 Me); 2.16 (m, 4 H, 2 allylic CH <sub>2</sub> ); 5.36 (s, 1 H, NH); 6.59 (s, 1 H, =CH)
	<sup>13</sup> C	21.39, 22.07, 24.11, 25.30 (4 C, 4 CH <sub>2</sub> ); 32.33 (2 C, 2 Me); 54.84 (1 C, C(Me) <sub>2</sub> ); 104.99 (1 C, ≡C); 133.34 (1 C, =CH); 133.84 (1 C, =C); 167.44 (1 C, CONH); 170.36 (1 C, ≡C); 187.72 (CO eq, Ru <sub>2,3</sub> ); <sup>b</sup> 189.19 (CO eq, Ru <sub>2,3</sub> ); <sup>b</sup> 194.00 (ν br CO, Ru <sub>1</sub> ); <sup>b</sup> 196.65 (CO <sub>ax</sub> , Ru <sub>2,3</sub> ) <sup>b</sup>
3b	<sup>1</sup> H	-21.03 (s, 1 H, μH); 2.00 (s, 6 H, 2 Me); 6.11 (br s, 1 H, NH); 7.43–7.51 (m, 5 H, Ph)
3c	<sup>1</sup> H	-23.52 (s, 1 H, μH); 1.59 (m, 4 H, 2 CH <sub>2</sub> ); 1.94 (s, 6 H, 2 Me); 2.19 (m, 4 H, 2 allylic CH <sub>2</sub> ); 5.66 (s, 1 H, NH); 6.59 (s, 1 H, =CH)
4a	<sup>1</sup> H	1.54 (s, 3 H, Me); 1.56–1.74 (m, 4 H, 2CH <sub>2</sub> ); 1.75 (s, 3 H, Me); 2.10–2.29 (m, 4 H, 2 allylic CH <sub>2</sub> ); 6.20 (s, 1 H, NH); 6.81 (m, 1 H, =CH); 10.96 (s, 1 H, =CH)
	<sup>13</sup> C	21.01, 21.79, 23.93, 25.93 (4 C, 4 CH <sub>2</sub> ); 33.01, 39.54 (2 C, 2 Me); 66.56 (1 C, C(Me) <sub>2</sub> ); 128.31 (1 C); 131.18 (1 C); 139.34 (1 C, CH); 162.79 (1 C, CH); 172.72 (1 C, CONH); 193.35 (1 C), 193.99 (2 C), 197.55 (2 C), 198.44 (2 C), 199.59 (1 C), 201.05 (1 C, RuCO) <sup>c</sup>
4b	<sup>1</sup> H	1.66 (s, 6 H, 2Me); 7.43–7.72 (m, 5 H, Ph); 11.0 (s, 1 H, =CH)

<sup>a</sup> CDCl<sub>3</sub>, 25 °C. <sup>b</sup> Ru<sub>1</sub> σ-bound to acetylide; Ru<sub>2,3</sub> π-bound to acetylide. <sup>c</sup> A fluxional process, involving some carbonyls, is probably occurring at room temperature, as a very broad band is observed between δ 195 and 200 under the sharp resonances reported above.

Table III. Experimental Data for the X-ray Diffraction Study on 4a

mol formula	C <sub>23</sub> H <sub>17</sub> NO <sub>12</sub> Ru <sub>4</sub> ·1/2CHCl <sub>3</sub>
mol wt	963.36
cryst syst	triclinic
space group	P $\bar{1}$
a, Å	13.521 (6)
b, Å	14.617 (6)
c, Å	9.049 (5)
α, deg	79.28 (2)
β, deg	108.79 (2)
γ, deg	111.85 (2)
V, Å <sup>3</sup>	1567 (1)
Z	2
D <sub>calcd</sub> , g cm <sup>-3</sup>	2.042
F(000)	926
cryst dimens, mm	0.18 × 0.23 × 0.27
linear abs, cm <sup>-1</sup>	20.42
diffractometer	Siemens AED
scan type	θ/2θ
scan speed, deg	3–12
scan width, deg	(θ–0.6) to (θ + 0.6 + 0.346 tan θ)
radiatn	Nb-filtered Mo Kα (λ = 0.71069 Å)
2θ range, deg	6–54
reflectns measd	±h, ±k, l
std reflectn	one measd after every 50 reflectns
no. of unique total data	6884
no. of unique obsd data	4586
[I > 2σ(I)]	
R	0.0426
R <sub>w</sub>	0.0478

was selected and mounted on the Siemens AED diffractometer for data collection. The crystallographic data are summarized in Table III. Unit cell parameters were determined from the θ values of 30 carefully centered reflections, having 12.1 < θ < 17.3°. Data were collected at room temperature, the individual profiles having been analyzed following Lehmann and Larsen.<sup>10</sup> The data

were corrected for the Lorentz and polarization effects.<sup>11</sup> No correction for the absorption effect was applied in view of the very low absorbance of the sample. Only the observed reflections were used in the structure solution and refinement.

The structure was solved by direct and Fourier methods and refined by full-matrix least-squares first with isotropic and then with anisotropic thermal parameters for all the non-hydrogen atoms excepting the carbon atoms of the cyclohexenyl ring and the chloroform molecule, found as solvation molecule. The cyclohexenyl ring was found in the "half-chair" conformation, but disordered, with the two carbons out of the plane distributed in two positions of equal occupancy factors. The hydrogen atoms, excepting those of the cyclohexenyl group, were clearly localized in the final difference Fourier map and refined isotropically. Those of the cyclohexenyl group were placed at their geometrically calculated positions and introduced in the final structure factor calculation with fixed isotropic thermal parameters. The chloroform molecule of solvation was found to be disordered and distributed close to the inversion center in two positions of equal occupancy factors, with a chlorine atom in common. The last cycles of refinement were carried out on the basis of 383 variables; at the end of the refinement no parameters shifted by more than 0.9 esd. The largest remaining peak in the final difference map was equivalent to about 0.77 e/Å<sup>3</sup>; unit weights were used in the first stages of the refinement, and then a weighting scheme,  $w = K[\sigma^2(F_o) + gF_o^2]^{-1}$ , was used, with  $K = 0.658$  and  $g = 0.013$  at the convergence. The analytical scattering factors, corrected for the real and imaginary parts of anomalous dispersions, were taken from ref 12. The final atomic coordinates for the non-hydrogen atoms are given in Table IV. The atomic coordinates of the

(11) Data reduction, structure solution, and refinement were carried out on the CRAY X-MP/12 computer of the Centro di Calcolo Elettronico Interuniversitario dell'Italia Nord-Orientale (CINECA, Casalecchio, Bologna, Italy) and on the Gould Powermode 6040 of the Centro di Studio per la Strutturistica Diffrattometrica del CNR, Parma, Italy, using the SHELX-76 system of crystallographic computer programs (Sheldrick, G. M. *Program for Crystal Structure Determination*; University of Cambridge: Cambridge, England, 1976).

(12) *International Tables for X-ray Crystallography*; Kynoch: Birmingham, England, 1974; Vol. IV.

(10) Lehmann, M. S.; Larsen, F. K. *Acta Crystallogr., Sect. A: Cryst. Phys. Diff., Theor. Gen. Crystallogr.* 1974, A30, 580.

Table IV. Fractional Atomic Coordinates ( $\times 10^4$ ) with Esd's in Parentheses for the Non-Hydrogen Atoms

atom	x	y	z
Ru(1)	2147 (1)	1510 (1)	1618 (1)
Ru(2)	4437 (1)	2543 (1)	2609 (1)
Ru(3)	3302 (1)	1101 (1)	4550 (1)
Ru(4)	3012 (1)	3535 (1)	2006 (1)
O(1)	1009 (6)	2459 (5)	-1383 (7)
O(2)	-69 (6)	32 (6)	1955 (8)
O(3)	2696 (7)	306 (7)	-242 (10)
O(4)	4503 (8)	3052 (7)	-780 (9)
O(5)	6565 (6)	4112 (6)	4236 (10)
O(6)	5713 (7)	1168 (7)	2886 (13)
O(7)	3359 (8)	4587 (5)	-1058 (8)
O(8)	4502 (6)	5451 (4)	3397 (7)
O(9)	3657 (8)	-562 (5)	3473 (10)
O(10)	4934 (6)	1273 (7)	7844 (8)
O(11)	1616 (6)	-593 (5)	5803 (10)
O(12)	1406 (4)	3733 (3)	1521 (6)
N	640 (5)	2472 (4)	3138 (7)
C(1)	1494 (6)	2163 (5)	-236 (8)
C(2)	761 (6)	592 (5)	1830 (8)
C(3)	2488 (7)	758 (7)	434 (10)
C(4)	4475 (8)	2895 (7)	478 (11)
C(5)	5796 (7)	3514 (6)	3627 (10)
C(6)	5206 (8)	1647 (7)	2848 (12)
C(7)	3240 (7)	4192 (5)	93 (9)
C(8)	3915 (6)	4736 (5)	2855 (8)
C(9)	3566 (8)	97 (6)	3852 (10)
C(10)	4350 (7)	1220 (6)	6625 (9)
C(11)	2239 (6)	72 (6)	5328 (10)
C(12)	3637 (5)	2699 (4)	4177 (7)
C(13)	2451 (5)	2269 (4)	3626 (7)
C(14)	1641 (5)	2415 (5)	4364 (7)
C(15)	1210 (6)	1544 (6)	5500 (8)
C(16)	2155 (7)	3368 (6)	5256 (9)
C(17)	568 (5)	3116 (5)	1894 (8)
C(18)	-555 (6)	3102 (5)	907 (9)
C(19)	-1548 (11)	2378 (10)	1239 (15)
C(20)	-2616 (19)	2731 (20)	416 (25)
C(202)	-2629 (18)	2268 (16)	-36 (35)
C(211)	-2673 (19)	2965 (18)	-1313 (25)
C(212)	-2615 (19)	3347 (17)	-620 (30)
C(22)	-1689 (13)	3800 (11)	-1465 (18)
C(23)	-631 (11)	3710 (9)	-343 (14)
Cl(1)	-808 (7)	4956 (6)	3424 (9)
Cl(2)	985 (11)	6857 (10)	4616 (15)
C(24)	655 (42)	5632 (35)	4851 (63)

hydrogen atoms are given in Table SI and the thermal parameters in Table SII in the supplementary material (see the paragraph at the end of the paper).

### Results and Discussion

The IR spectra of the complexes **3** are closely comparable to that of **2**;<sup>4a</sup> in all the spectra of **3** and **4** strong (and sometimes broad) signals around 1650  $\text{cm}^{-1}$  indicate the presence of an amide C=O and hence of ligand A or B.

The  $^1\text{H}$  NMR spectra of complexes **3** clearly show the presence of a hydridic hydrogen with chemical shift very close to that observed for **2**; the other signals and their relative intensities are those expected for the nature of the ligands. On the basis of these results, we consider the complexes **3a-c** to have structures comparable to that of the hydridoacetylide complex **2**; the room-temperature  $^{13}\text{C}$  NMR spectrum of **3a** is in accord with this hypothesis and indicates only localized scrambling for some COs, probably those on the Ru atom  $\sigma$ -bonded to the acetylide. Similar results had been obtained for complex **2**.<sup>13</sup>

In the  $^1\text{H}$  NMR spectra of the complexes **4**, the very low field signals (10.96 and 11.00 ppm) have been attributed to the terminal hydrogen of the acetylene; the carbon atom

Table V. Important Interatomic Distances (Å) and Angles (deg) for **4a**

Ru(1)-Ru(2)	2.811 (1)	C(14)-C(16)	1.554 (11)
Ru(1)-Ru(3)	2.696 (1)	N-C(14)	1.467 (8)
Ru(2)-Ru(3)	2.798 (1)	N-C(17)	1.328 (9)
Ru(1)-Ru(4)	2.793 (1)	O(12)-C(17)	1.258 (8)
Ru(2)-Ru(4)	2.687 (1)	C(17)-C(18)	1.488 (10)
Ru(1)-C(1)	1.893 (7)	C(18)-C(19)	1.448 (15)
Ru(1)-C(2)	1.901 (7)	C(18)-C(23)	1.303 (14)
Ru(1)-C(3)	1.924 (12)	C(1)-O(1)	1.140 (9)
Ru(1)-C(13)	2.152 (7)	C(2)-O(2)	1.142 (10)
Ru(2)-C(4)	1.914 (10)	C(3)-O(3)	1.135 (17)
Ru(2)-C(5)	1.922 (7)	C(4)-O(4)	1.129 (13)
Ru(2)-C(6)	1.899 (12)	C(5)-O(5)	1.133 (10)
Ru(2)-C(12)	2.127 (8)	C(6)-O(6)	1.140 (17)
Ru(3)-C(9)	1.887 (12)	C(7)-O(7)	1.122 (11)
Ru(3)-C(10)	1.946 (7)	C(8)-O(8)	1.134 (8)
Ru(3)-C(11)	1.864 (8)	C(9)-O(9)	1.139 (15)
Ru(3)-C(12)	2.189 (6)	C(10)-O(10)	1.128 (10)
Ru(3)-C(13)	2.290 (7)	C(11)-O(11)	1.144 (10)
Ru(4)-C(7)	1.876 (8)	C(19)-C(20)	1.62 (3)
Ru(4)-C(8)	1.862 (6)	C(19)-C(202)	1.52 (2)
Ru(4)-C(12)	2.208 (6)	C(22)-C(23)	1.50 (2)
Ru(4)-C(13)	2.193 (6)	C(22)-C(211)	1.46 (3)
Ru(4)-O(12)	2.191 (6)	C(22)-C(212)	1.55 (3)
C(12)-C(13)	1.437 (8)	C(201)-C(211)	1.52 (3)
C(13)-C(14)	1.545 (12)	C(202)-C(212)	1.56 (3)
C(14)-C(15)	1.537 (9)		
Ru(2)-Ru(1)-Ru(3)	61.0 (1)	Ru(4)-O(12)-C(17)	125.7 (5)
Ru(2)-Ru(1)-Ru(4)	57.3 (1)	C(14)-N-C(17)	127.9 (6)
Ru(1)-Ru(2)-Ru(3)	57.5 (1)	O(12)-C(17)-N	122.9 (7)
Ru(1)-Ru(2)-Ru(4)	61.0 (1)	N-C(17)-C(18)	118.2 (7)
Ru(1)-Ru(3)-Ru(2)	61.5 (1)	O(12)-C(17)-C(18)	118.9 (6)
Ru(1)-Ru(4)-Ru(2)	61.7 (1)	N-C(14)-C(13)	109.8 (5)
C(1)-Ru(1)-C(2)	93.6 (4)	N-C(14)-C(15)	104.4 (6)
C(1)-Ru(1)-C(3)	91.4 (4)	N-C(14)-C(16)	108.2 (6)
C(1)-Ru(1)-C(13)	110.4 (3)	C(13)-C(14)-C(15)	113.7 (6)
C(2)-Ru(1)-C(3)	99.1 (4)	C(13)-C(14)-C(16)	112.8 (6)
C(2)-Ru(1)-C(13)	93.8 (3)	C(15)-C(14)-C(16)	107.5 (6)
C(4)-Ru(2)-C(5)	99.8 (4)	Ru(1)-C(1)-O(1)	172.5 (7)
C(4)-Ru(2)-C(6)	91.2 (5)	Ru(1)-C(2)-O(2)	179.2 (8)
C(5)-Ru(2)-C(6)	90.1 (5)	Ru(1)-C(3)-O(3)	178.8 (8)
C(5)-Ru(2)-C(12)	90.7 (3)	Ru(2)-C(4)-O(4)	176.1 (9)
C(9)-Ru(3)-C(10)	100.1 (4)	Ru(2)-C(5)-O(5)	176.4 (9)
C(9)-Ru(3)-C(11)	85.5 (4)	Ru(2)-C(6)-O(6)	173.5 (10)
C(10)-Ru(3)-C(11)	90.7 (4)	Ru(4)-C(7)-O(7)	178.8 (10)
C(10)-Ru(3)-C(12)	92.2 (3)	Ru(4)-C(8)-O(8)	177.0 (8)
O(12)-Ru(4)-C(7)	93.2 (3)	Ru(3)-C(9)-O(9)	174.6 (9)
O(12)-Ru(4)-C(8)	98.2 (3)	Ru(3)-C(10)-O(10)	178.1 (9)
C(7)-Ru(4)-C(8)	85.5 (3)	Ru(3)-C(11)-O(11)	176.3 (8)

bearing this hydrogen is bound either  $\sigma$  or  $\pi$  to the metal atoms. This attribution is based on previous experience on comparable complexes.<sup>1,14</sup> The  $^{13}\text{C}$  NMR spectrum of **4a** would indicate stereochemical rigidity at room temperature of the ligand moiety; this is of particular interest as the complex lacks of symmetry planes and inversion center and, hence, is a chiral molecule.

**X-ray Structure of  $\text{Ru}_4(\text{CO})_{11}(\text{HC}\equiv\text{CCMe}_2\text{NHCOC}_6\text{H}_9)$  (**4a**).** The structure of the tetranuclear complex **4a** is depicted in Figure 1; the most important bond distances and angles are given in Table V. The structure consists of a butterfly arrangement of ruthenium atoms bonded to 11 terminal CO groups and to the organic molecule through the C-C triple bond and the amide oxygen atom. Three Ru atoms are bound each to three CO groups, whereas the fourth one, Ru(4), is bound to only two CO groups, interacting also with the amide oxygen atom. The Ru-Ru metal-metal bonds, in the range 2.687 (1)-2.811 (1) Å, and the dihedral angle between the two wings, 113.3 (1)°, are typical of this class of ruthenium butterfly clusters bound to alkynes.<sup>6</sup> The alkyne interacts

(13) Aime, S.; Milone, L.; Gambino, O.; Sappa, E.; Rosenberg, E. *Inorg. Chim. Acta* 1975, 15, 53.

(14) Aime, S.; Milone, L.; Sappa, E. *J. Chem. Soc., Dalton Trans.* 1976, 838. Aime, S.; Milone, L.; Sappa, E. *Inorg. Chim. Acta* 1976, 16, L7.

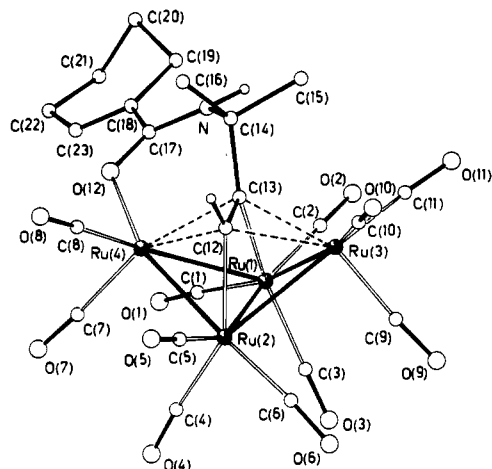
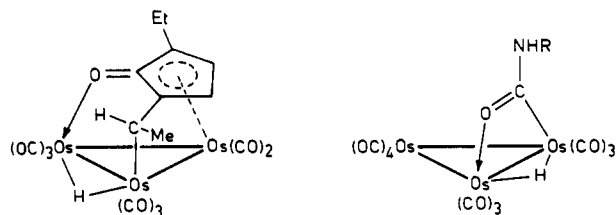


**Figure 1.** View of the structure of **4a** with the atomic labeling scheme.

with all the four metals, being  $\sigma$ -bound to the hinge Ru(1) and Ru(2) atoms and  $\pi$ -bound to the wingtip Ru(3) and Ru(4) atoms, and is disposed with the C(12)–C(13) triple bond nearly parallel to the hinge edge. Also the C(12)–C(13) bond distance, 1.437 (8) Å, is in the common range found in similar derivatives.<sup>6</sup>

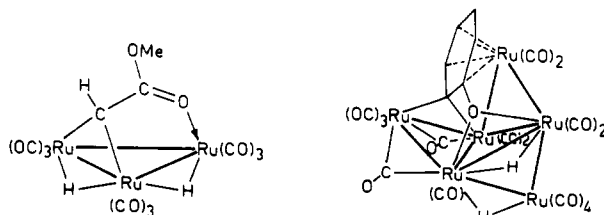
An additional interaction involves the wingtip Ru(4) atom with the amide oxygen atom, the Ru(4)–O(12) bond distance being 2.191 (6) Å. The interaction of one cluster metal with an oxygen atom of an organic CO group, although here reported for the first time, to our knowledge, for a butterfly cluster, is not uncommon in ruthenium and osmium carbonyl cluster chemistry. Thus, in 1977 Shapley and co-workers reported the pyrolytic synthesis of  $(\mu\text{-H})\text{Os}_3(\text{CO})_8[\text{C}(\text{=O})\text{C}(\text{CHMe})\text{CHCHC}(\text{Et})]$  (**5**),<sup>15</sup> and in 1980 Deeming reported some of the first terms of a cluster class well-known at present, namely, those where a (R)–C=O ligand bridges two metal atoms; in particular  $(\mu\text{-H})\text{Os}_3(\text{CO})_{10}[(\mu\text{-PhMeHCNHC}(\text{O}))]$  (**6**) was described, among others.<sup>16</sup>



(5)

(6)

When restricting the discussion to ruthenium clusters only, noteworthy are  $(\mu\text{-H})_2\text{Ru}_3(\text{CO})_9(\mu_3\text{-}\eta^2\text{-CHCOOMe})$  (**7**)<sup>17</sup> and the "raft" cluster  $\text{H}_2\text{Ru}_6(\text{CO})_{16}(\text{C}_6\text{H}_4\text{O})$  (**8**), where



(7)

(8)

(15) Churchill, M. R.; Lashewycz, R. A.; Takikawa, M.; Shapley, J. R. *J. Chem. Soc., Chem. Commun.* 1977, 699.

(16) Arce, A. J.; Deeming, A. J. *J. Chem. Soc., Chem. Commun.* 1980, 1102.

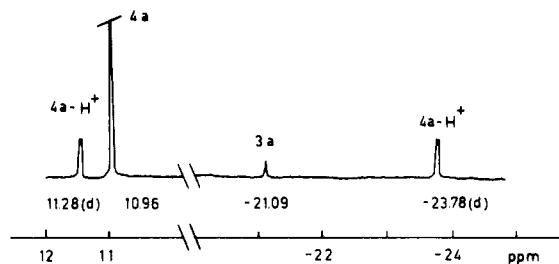
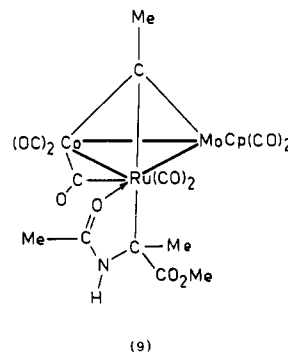


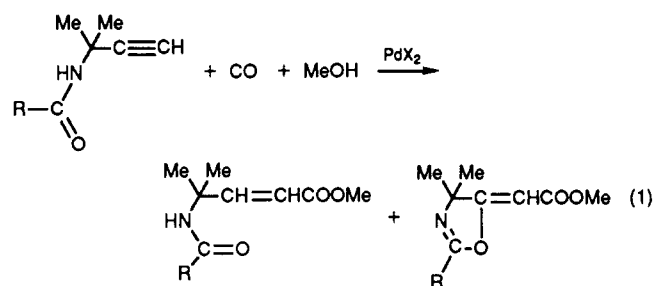
**Figure 2.**  $^1\text{H}$  NMR spectrum of a  $\text{CDCl}_3$  solution of **4a**, a few minutes after the addition of an excess of  $\text{CF}_3\text{COOH}$ :  $4\text{a-H}^+$  = protonated **4a**; d = doublet.

the phenoxy ligand is coordinated to three of the Ru atoms in an edge-bridged butterfly arrangement and the oxygen atom bridges two metal centers.<sup>18</sup> The complex **8** is involved in hydrogen-transfer reactions. Even more interesting is the product of the reaction of the chiral cluster  $(\mu_3\text{-RC})\text{RuCoM}(\text{Cp})(\text{CO})_8\text{H}$  (R = Me, Ph; M = Mo, W) with the prochiral alanine precursors acetamide acrylic acid methyl ester; in the product  $(\mu_3\text{-RC})\text{RuCoM}(\text{Cp})(\text{CO})_7[(\text{Me})(\text{CCOMe})\text{CNHC}(\text{OMe})]$  (**9**) the CO oxygen interacts with the Ru atom rather than with one of the other metals, which also show affinity for oxygen.<sup>19</sup>



(9)

Some considerations should be added concerning the significance of the acetylenic amide arrangement in the butterfly cluster as a model for pathways observed in catalytic reactions. We observed that in the presence of a palladium chloride–thiourea catalyst a carbomethoxylation reaction of simple alkynes, such as 1-hexyne, is difficult and slow; in contrast, if an amido group is present in the alkyne molecule in a favorable position to coordinate to the metal, the reaction proceeds smoothly to give carbonylation products (eq 1).<sup>5</sup>



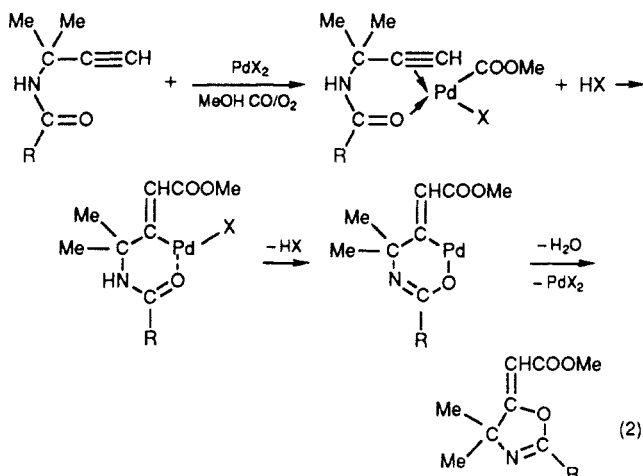
The oxazoline product implies that the amido group was in the correct position for a chelating metallacycle arrangement involving an amide CO–metal interaction similar to that found in the present work. In the presence of

(17) Churchill, M. R.; Janik, T. S.; Duggan, T. P.; Keister, J. B. *Organometallics* 1987, 6, 799.

(18) Bhaduri, S.; Sharma, K.; Jones, P. G. *J. Chem. Soc., Chem. Commun.* 1987, 1769.

(19) Mani, D.; Schacht, H.-T.; Powell, A.; Vahrenkamp, H. *Organometallics* 1987, 1360.

palladium the carbonylation reaction could take place catalytically, whereas the ruthenium complex, under the mild conditions used, is too stable to lead to the same products. Nevertheless, this ruthenium complex can provide evidence for the model of the palladium-assisted carbonylation reaction (eq 2).



**Some Comments on the Formation of the Clusters 4 and on Their Protonation Reactions.** The unexpected metal fragment condensation observed for  $\text{Ru}_3(\text{CO})_{12}$  in the presence of ligands A and B, which are terminal alkynes,<sup>20</sup> to give complexes 4 led us to investigate the formation pathways of these clusters; as a first step, we could show that clusters 4 are not formed by simple thermal treatment of the very stable clusters 3.

As for other alkyne-substituted tetranuclear homo- and heterometallic clusters obtained from trinuclear precursors, two main routes may be expected, that is, (i) formation of tetrahedral "precursors" such as  $\text{H}_4\text{Ru}_4(\text{CO})_{12}$  or better  $\text{H}_2\text{Ru}_4(\text{CO})_{13}$ , which then undergo metal-metal bond cleavage in the presence of alkynes<sup>1,6</sup> to give the butterfly cluster, or (ii) the "trapping" of  $\text{Ru}(\text{CO})_x$  fragments from alkynes already coordinated to three-metal centers. If we exclude route i, which would require a source of hydrogen, we must invoke pathway ii, and in fact complex 3a easily reacts with excess  $\text{Ru}_3(\text{CO})_{12}$  (as a source of  $\text{Ru}(\text{CO})_x$ ) to give moderate yields of 4a. The low yields of 4c are also explainable, as  $\text{Os}_3(\text{CO})_{12}$  shows a very low tendency to give fragments in solution.

Addition of an excess of  $\text{CF}_3\text{CO}_2\text{H}$  to a  $\text{CDCl}_3$  solution of 4a at room temperature gives after few minutes a  $^1\text{H}$  NMR spectrum containing new peaks at  $\delta$  -21.09 s, -23.78 d, and 11.28 d ( $^3J_{\text{HH}} = 1.5$  Hz), which slowly increase

during time. The latter two peaks are related by the same coupling constant and the same integrated area; at this stage, their area is 4 times greater than that of the other hydride at  $\delta$  -21.09 ppm but almost 10 times smaller than that of the starting alkyne proton at  $\delta$  10.96 (see Figure 2). After more time, a gradual decrease of the peaks at  $\delta$  -23.78 and 11.28 (which remain related) and of the alkyne peak of the parent complex occurs and is accompanied by a corresponding raise of the other hydride peak at  $\delta$  -21.09. The latter, after 14 h, appears the major one-proton peak and after 2 days is only one-proton peak, the other alkyne and hydride signals disappearing. Only minor modifications are observed for the other signals, and the solution turns from red to yellow, giving some decomposition products.

The above results may be explained by considering that, in agreement with previous results,<sup>21</sup> a slow proton transfer takes place to a Ru-Ru edge ( $\delta$  -23.78 d,  $^3J_{\text{HH}} = 1.5$  Hz) close to the alkyne proton which, therefore, is slightly deshielded ( $\delta$  11.28 d). This fact, along with the protonation of the amide moiety (NH peaks at lower field), which should produce a weakening of the  $\text{NHCO}\cdots\text{Ru}$  interaction, causes destabilization of the *closo*- $\text{Ru}_4\text{C}_2$  core, which turns into the hydridoacetylido cluster 3a by alkyne deprotonation and by loss of a  $\text{Ru}(\text{CO})_2$  fragment. The formation of the trinuclear cluster 3a is supported by the presence of its characteristic  $^1\text{H}$  signals at  $\delta$  -21.09, 1.92, and 1.62, unaffected by the likely protonation of the dangling amide group.

Thus, by protonation, the reverse process observed in the thermal synthesis of 4a occurs, that is, the metal fragment loss involving the amide group which seems responsible for the pickup of the same fragment, during tetranuclear cluster condensation.

Further studies on the reactivity of functionalized alkynes toward metal clusters are in progress in our laboratories.

**Acknowledgment.** We gratefully thank the Italian Ministero della Pubblica Istruzione and the Commission of the European Communities (contract No. ST 2J-0347-C) for financial supports.

**Registry No.** 3a, 126823-23-2; 3b, 126823-22-1; 3c, 126823-26-5; 4a, 126823-24-3; 4a- $^{1/2}\text{CHCl}_3$ , 126823-29-8; 4b, 126823-25-4; 4c, 126823-27-6;  $\text{HC}\equiv\text{CCMe}_2\text{NHCOC}_6\text{H}_9$ , 126823-21-0;  $\text{HC}\equiv\text{CCMe}_2\text{NHCOPh}$ , 7471-09-2;  $\text{Ru}_3(\text{CO})_{12}$ , 15243-33-1;  $\text{Os}_3(\text{CO})_{12}$ , 15696-40-9.

**Supplementary Material Available:** Table SI, coordinates and isotropic thermal parameters for the hydrogen atoms, and Table SII, thermal parameters for the non-hydrogen atoms (35 pages); a listing of observed and calculated structure factors (26 pages). Ordering information is given on any current masthead page.

(21) Johnson, B. F. G.; Lewis, J.; Schorpp, K. T. *J. Organomet. Chem.* 1975, 91, C13.

(20) Metal fragment condensation in the presence of terminal alkynes has indeed been reported, but in a few examples only; two of them are in: Sappa, E.; Tiripicchio, A.; Camellini, M. *J. Chem. Soc., Dalton Trans.* 1978, 419. Aime, S.; Nicola, G.; Osella, D.; Manotti Lanfredi, A. M.; Tiripicchio, A. *Inorg. Chim. Acta* 1984, 85, 161.